



HAL
open science

The impact of Neurofeedback on effective connectivity networks in chronic stroke patients: an exploratory study

Giulia Lioi, Adolfo Veliz, Julie Coloigner, Quentin Duché, Simon Butet, Mathis Fleury, Emilie Leveque-Le Bars, Elise Bannier, Anatole Lécuyer, Christian Barillot, et al.

► To cite this version:

Giulia Lioi, Adolfo Veliz, Julie Coloigner, Quentin Duché, Simon Butet, et al.. The impact of Neurofeedback on effective connectivity networks in chronic stroke patients: an exploratory study. *Journal of Neural Engineering*, 2021, 18 (5), pp.056052. 10.1088/1741-2552/ac291e . hal-03354296

HAL Id: hal-03354296

<https://imt-atlantique.hal.science/hal-03354296v1>

Submitted on 19 Nov 2021

HAL is a multi-disciplinary open access archive for the deposit and dissemination of scientific research documents, whether they are published or not. The documents may come from teaching and research institutions in France or abroad, or from public or private research centers.

L'archive ouverte pluridisciplinaire **HAL**, est destinée au dépôt et à la diffusion de documents scientifiques de niveau recherche, publiés ou non, émanant des établissements d'enseignement et de recherche français ou étrangers, des laboratoires publics ou privés.

1 Title

2 **The Impact of Neurofeedback on Effective Connectivity Networks in Chronic Stroke Patients: an**
3 **exploratory study**

4 Authors

5 Lioi Giulia^{1,4*§}, Veliz Adolfo^{1§}, Coloigner Julie¹, Duché Quentin^{1,2}, Butet Simon², Mathis Fleury¹, Emilie
6 Leveque-Le Bars², Elise Bannier^{1,3}, Anatole Lécuyer¹, Christian Barillot^{1†}, Isabelle Bonan^{2†}

7 1 Univ Rennes, Inria, CNRS, Inserm, IRISA, Rennes, France

8 2 CHU Rennes, Departement of Physical and Rehabilitation Medicine, Rennes, France

9 3 CHU Rennes, Departement of Radiology, Rennes, France

10 4 IMT Atlantique, Lab-STICC, UMR CNRS 6285, F-29238, France

11 *corresponding author giulia.lioi@imt-atlantique.fr

12 §These authors have contributed equally to the work

13 † These authors have contributed equally to the work

14 Keywords

15 **Neurofeedback, Effective Connectivity, Stroke Rehabilitation, Dynamic Causal Modeling, fMRI**

16 Abstract

17

18 Objective

19 In this study, we assessed the impact of EEG-fMRI Neurofeedback (NF) training on connectivity strength
20 and direction in bilateral motor cortices in chronic stroke patients. Most of the studies using NF or brain
21 computer interfaces for stroke rehabilitation have assessed treatment effects focusing on successful
22 activation of targeted cortical regions. However, given the crucial role of brain network reorganization
23 for stroke recovery, our broader aim was to assess connectivity changes after a NF training protocol
24 targeting localised motor areas.

25

26 Approach

27 We considered changes in fMRI connectivity after a multisession EEG-fMRI NF training targeting
28 ipsilesional motor areas in nine stroke patients. We applied the Dynamic Causal Modeling and
29 Parametric Empirical Bayes frameworks for the estimation of effective connectivity changes. We
30 considered a motor network including both ipsilesional and contralesional premotor, supplementary
31 and primary motor areas.

32

33 Main results

34 Our results indicate that NF upregulation of targeted areas (ipsilesional supplementary and primary
35 motor areas) not only modulated activation patterns, but also had a more widespread impact on fMRI
36 bilateral motor networks. In particular, inter-hemispheric connectivity between premotor and primary
37 motor regions decreased, and ipsilesional self-inhibitory connections were reduced in strength,
38 indicating an increase in activation during the NF motor task.

39

40 Significance

41 To the best of our knowledge, this is the first work that investigates fMRI connectivity changes elicited
42 by training of localized motor targets in stroke. Our results open new perspectives in the understanding
43 of large-scale effects of NF training and the design of more effective NF strategies, based on the
44 pathophysiology underlying stroke-induced deficits.

45

46 Introduction

47 A growing body of evidence suggests that post-stroke motor deficits are related to altered interactions
48 between brain areas also remote from the stroke lesion [1]. Indeed, localized structural lesions resulting
49 from stroke are likely to affect brain connectivity through the brain. As a consequence, recovery from
50 stroke depends on structural and functional networks reorganization [2]–[5]. These findings are in line
51 with the increasingly influential thesis that most of complex biological diseases, such as motor disorders
52 [1], psychiatric disorders [6] or Alzheimer disease [7] are related to the dysfunction of complex brain
53 networks [8].

54 In stroke in particular, several studies have used brain functional neuroimaging techniques such as
55 positron emission tomography (PET), functional Magnetic Resonance imaging (fMRI) and
56 electroencephalography (EEG) to investigate changes in brain activity [9], [10]. More recently,
57 connectivity-based analyses have shed new light into the pathophysiology underlying stroke-induced
58 deficits [4], [11], [12]. A general trend observed in these studies is that stroke induces changes in both
59 hemispheres and causes a disruption of ipsilesional connectivity [13]. Some of these connectivity-based
60 approaches have gone further and investigated the effect of interventions (such as physical or robotic
61 assisted therapy) on cortical network reorganization, and its link to motor function recovery [14].
62 However, the impact of specific therapies on motor connectivity in stroke remains to be investigated.
63 Assessment of changes in connectivity networks induced by treatment is now considered to be a
64 promising way to individualize therapies and enhance rehabilitation outcome after stroke [1].

65 There are different ways of estimating brain connectivity from neuroimaging data. Structural
66 connectivity refers to anatomical connections between brain regions and is most commonly estimated
67 using Diffusion Tensor Imaging (DTI). Functional connectivity (FC) is defined as the statistical
68 dependence among measurements of neural activity [15] and it is usually inferred through correlations
69 among neurophysiological signals. Effective connectivity (EC) estimates the influence that one neuronal
70 system exerts on another. EC is intrinsically directed, but does not necessarily imply a direct coupling
71 mediated by anatomical connections. Connectivity studies in stroke have relied both on FC [16], [17]
72 and EC [3], [18], [19]. Among EC estimators, those based on Dynamic Causal Modeling (DCM) are
73 particularly robust for fMRI data analysis, while lag-based approach (i.e. Granger causality) may perform
74 poorly if the hemodynamic effects are not properly taken in account [20].

75 Among the set of therapies proposed for stroke rehabilitation, Neurofeedback (NF) is gaining increasing
76 attention since it potentially promotes plasticity of perilesional areas by means of brain self-regulation.
77 Recent works have investigated the potential of NF (or Brain Computer Interfaces, BCI) for motor
78 rehabilitation after stroke as an alternative or in addition to traditional physical therapies [21]–[25]. In
79 these studies, patients perform motor imagery (MI) of the affected limb, which is a promising mental
80 therapy to restore motor activation. Even if there is no clinical evidence of the benefit of NF over MI for

81 stroke rehabilitation, NF was shown to enhance the efficacy of MI training, by eliciting more specific
82 brain patterns [26], [27]. In some applications, the NF paradigm allows to integrate the feedback in an
83 orthosis to support the movement of the affected limb, thus closing the sensorimotor loop [28], [29].

84 The majority of these NF approaches have relied on one imaging technique, mainly
85 electroencephalographic (EEG) recordings. EEG-NF applications are generally based on the training of
86 sensorimotor rhythms in motor regions ipsilateral to the stroke lesion [30]–[32]. Similarly, more recent
87 fMRI-NF studies have promoted upregulation of ipsilesional motor areas or motor system connectivity
88 [23], [33]–[35]. Building on the pioneering work of Zotev and collaborators [36], [37], we integrated
89 EEG and fMRI for bimodal NF for motor training, with the rationale of providing a more specific
90 feedback, combining high temporal (EEG) and spatial (fMRI) resolution [38]. We have also shown the
91 feasibility of EEG-fMRI NF and its potential to promote upregulation of ipsilesional motor regions in a
92 pilot study involving chronic stroke patients [24]. In this previous work, we have investigated NF training
93 effects focusing on the activation of localized target cortical areas. In the present study, we characterize
94 global changes elicited by NF training on EC networks in chronic stroke patients undergoing a longer NF
95 training protocol. We assessed fMRI connectivity changes using a DCM approach and considered a
96 motor network including bilateral premotor, supplementary and primary motor areas (PMC, SMA, M1).
97 We believe that our results bring new insight into large-scale effects of NF training in stroke and on the
98 potential of NF in driving maladaptive networks reorganization.

99 **Methods**

100 *Participants*

101 Nine chronic stroke patients (mean age 59 years, age range: 37-77 years, 3 females) were included in
102 the study. Patients had mild to severe hemiparesis of the upper limb (Upper extremity Fugl-Meyer score
103 in the range 26-55) with variable lesion characteristics (Table 1) but were clinically stable, at more than
104 one year from the stroke episode (33.2 ± 16.5 months). Integrity of the corticospinal tract (CST) was an
105 inclusion criterion. Patients for whom the CST fractional anisotropy asymmetry index exceeded the 0.15
106 threshold [39] were not enrolled. More details about diffusion imaging processing and CST
107 segmentation are given in Supplementary Material. This study is part of a larger randomized controlled
108 study to assess the efficacy of NF (NCT03766113). In this exploratory work, we considered a subsample
109 of participants with the aim of validating data quality and investigating the effect of NF training on motor
110 connectivity. All participants gave their written informed consent and the study was approved by the
111 institutional review board and registered.

112 *Experimental Protocol*

113 Participants underwent a NF protocol alternating bimodal EEG-fMRI NF (N=5) and unimodal EEG-NF
114 sessions (N=9) over a period of five weeks. NF sessions included a calibration and three NF training
115 blocks alternating epochs of rest (20 s) and NF-MI training (20 s) (Figure S1). Patients were informed at
116 inclusion, verbally and by an explanatory note, about the goals and the timeline of the study.
117 Instructions were repeated before each training session and oriented the patients towards a kinesthetic
118 MI of the affected upper limb, without mentioning a specific strategy.

119 Imaging was performed using a Siemens 3T Prisma scanner running VE11C and a 64-channel MR-
120 compatible EEG system from Brain Products (Brain Products GmbH, Gilching, Germany). Functional MRI
121 data were acquired with echo-planar imaging (EPI) with the following parameters: repetition time

122 (TR)/echo time (TE) = 1,000/23 ms, FOV = 230 × 230 mm², 16 4-mm slices, voxel size = 2.2 × 2.2 × 4 mm³,
123 matrix size = 105 × 105, flip angle = 90°. For each session, a high-resolution 3D T1 MPRAGE sequence
124 was acquired with the following parameters: TR/TI/TE = 1,900/900/2.26 ms, parallel imaging with
125 GRAPPA 2, FOV = 256 × 256 mm² and 176 slabs, voxel size = 1 × 1 × 1 mm³, flip angle = 9°. In order to
126 assess the asymmetry between the ipsilesional and contralesional CST, diffusion imaging
127 (TR/TE=11000/99ms, FOV 256x256mm², 60 slices, matrix 128x128, voxel size, 2x2x2 mm³, 30 directions,
128 b=1000s/mm²) was performed before inclusion. During rest, a cross was displayed on the screen and
129 participants were asked to concentrate on the cross and rest. During the task, a visual feedback in the
130 form of a ball moving in a one-dimensional gauge proportionally to the average of the EEG and the fMRI
131 features was presented. More specifically, the bimodal NF was calculated as the normalized average of
132 the EEG- NF score (Event Related Desynchronization in the 8-30 Hz band of 18 motor electrodes,
133 updated every 250 ms) and fMRI NF score (weighted sum of the difference between percentage signal
134 change in the two ROIs (SMA and M1) and a large deep background region, updated every TR=1 s), as
135 explained in more detail in the supplementary material. Unimodal EEG-NF sessions were performed
136 using the Mensia Modulo (MENSIA TECHNOLOGIES) hardware solution, equipped with an 8-channel
137 EEG cap. Patients were exposed to the same feedback metaphor on a computer screen. More details
138 about the NF platform performing real-time EEG-fMRI processing, the unimodal NF sessions and the
139 experimental protocol are given in [24], [38], [40] and in the attached Supplementary Material.

140 *Calibration and online NF calculation*

141 At the beginning of each training session, a MI task without NF was performed to calibrate the fMRI
142 signal. Functional MRI data were pre-processed for motion correction and slice-time correction and
143 realigned with the structural scan. After spatial smoothing with a 6 mm FWHM Gaussian kernel, a
144 general linear model (GLM) analysis was performed. The calibration activation map was used to define
145 two regions of interest (ROIs) to calculate NF scores for the subsequent NF task. Boxes of 9x9x3 voxels
146 (20×20×12 mm³) centered on the peak of activation in the ipsilesional SMA and M1 were considered.
147 As detailed in a previous work [24], we proposed an adaptive rewarding strategy that more importantly
148 weighted SMA at the beginning of the training and then guided the patients towards activation of the
149 ipsilesional M1. The rationale behind this adaptive NF training is that ipsilesional M1 is considered the
150 ideal target for motor recovery. However, while SMA seems to be more robustly and easily recruited
151 during MI, M1 activation during MI is more difficult to achieve [41], [42]. The proposed NF reinforcement
152 scheme aims at gradually guiding the patients towards the activation of the ipsilesional primary motor
153 cortex, while first engaging more importantly the supplementary motor areas. The fMRI NF score was
154 therefore calculated as a weighted combination of the activity in the SMA and M1 ROIs, with weights
155 changing at each training session. In particular the fMRI-NF score was calculated as the difference
156 between percent signal change in the two ROIs (SMA and M1) and a background slice whose activity is
157 not correlated with the NF task, in order to reduce the impact of global signal changes [43].

158 For the sake of brevity of this manuscript focusing on fMRI effective connectivity analysis, we have
159 provided more details about calibration and NF calculation procedure in Supplementary Material. A
160 CRED-nf checklist with details about experimental design [44] is also available as Supplementary File 1
161 together with a table summarizing real-time signal processing steps, according to the COBIDAS-inspired
162 template [45] (Table S1, Supplementary Material).

163 *fMRI preprocessing*

164 In order to assess the effect of the multi-session NF training protocol on EC patterns, we considered
165 fMRI time-series of the first (b-s1) and last (b-s5) bimodal NF training sessions. BOLD series were pre-
166 processed and processed with Matlab and SPM12 (Wellcome Department of Imaging Neuroscience,
167 UCL, London, UK). A slice timing correction was applied to correct for timing differences within volumes.
168 Functional volumes were then registered to the mean volume to compensate for subject motion within
169 the series and ensure voxel-to-voxel correspondence across time. The mean fMRI image was co-
170 registered with the subject structural image. The anatomical volume was in turn segmented and non-
171 linearly transformed to the reference Montreal Neurological Institute (MNI) space. The estimated
172 normalization deformations fields were later applied to functional data that were finally smoothed using
173 a 3D Gaussian kernel of 6 mm FWHM.

174 An offline data quality control was performed to assess for the impact of head movement artifacts on
175 data quality and NF performances. Motion parameters were estimated and used to perform a post-hoc
176 correlation analysis with the NF task. To this end and for each bimodal session a Framewise
177 Displacement (FD) was computed from the six realignment parameters as proposed by Power et al. [46].
178 FD outliers were identified using the spmup tool within the QAP Package [47]. Pearson correlation
179 analysis between the FD time-series and the NF task was assessed.

180 At the subject level, each session was modeled using a three-run generalized linear model (GLM), where
181 each NF block and each rest block were modeled by convoluting a 20s boxcar function with the standard
182 hemodynamic response function (HRF) to build a NF task and a rest regressors. The estimated motion
183 parameters and a run mean were also entered in the design matrix as covariates of no interest. NF
184 blocks and rest blocks were contrasted run-wise in order to analyze the NF effect session-wise but also
185 averaged over the three runs to evaluate the NF effect over the whole bimodal session. The normalised
186 individual contrast maps of the three patients with right lesions were flipped along the y axis to create
187 an artificial group of 9 patients with left-only hemispheric lesions. These maps were entered into a
188 training session specific second level analysis GLM to evaluate group activation maps at each NF training
189 session, allowing to monitor the effect of NF on brain activation.

190 The evolution of the NF effect over bimodal sessions was evaluated within a two-step procedure at both
191 the individual and group level. At the individual level, individual NF-rest contrast maps were entered in
192 the design matrix. At the group level, NF-rest group contrast maps obtained from the previous GLM
193 analysis were entered in the design matrix. In both cases, 14 session-wise NF-rest contrast maps were
194 entered in the first column of the linear increase design matrix. A time regressor ranging from 1 to 14
195 coding for the NF session index was added as a second column. By contrasting the effect of time,
196 resulting statistical maps provided voxels or clusters demonstrating a linear increase (or decrease) of
197 (group or individual) brain activity over the NF sessions.

198 *ROI definition and time series extraction*

199 In order to discard task independent noise, representative time series for the selected ROIs were
200 extracted by considering the voxels which, in the first level GLM analysis, exceeded the statistical
201 threshold for NF contrast ($p < 0.01$), and were located within an a priori mask for bilateral SMA, PMC and
202 M1. These masks were defined using the Human Motor Area Template (HMAT) atlas [48]. The SMA
203 mask included both preSMA and SMA HMAT ROIs, and the PMC included ventral and dorsal PMC. To
204 adapt the selected ROIs to individual responses, we extracted the first principal component of the time
205 series from all voxels within 8-mm spheres around local activation maxima [49]. As for whole brain

206 analysis, ROIs time series were flipped in the case of patients with a right hemisphere lesion (N=3) for
207 the sake of the group analysis (in the group results of the affected hemisphere is thus presented on the
208 left).
209

210 *Dynamical causal modeling (DCM)*

211 DCM is a hypothesis-based technique that describes how observed fMRI responses are generated using
212 a set of differential equations and represents one of the most common frameworks for the analysis of
213 fMRI effective connectivity [50]. These differential equations describe how experimental stimulation
214 (input) produces changes in neural activity and induces changes in the output (i.e. the observed fMRI
215 data) through a hemodynamic model [51]. DCM models include parameters, such as the strength of
216 coupling between the ROIs, i.e. effective connectivity, which are estimated from the data using a
217 variational Laplace approach [52].

218 In the current DCM study, we assessed the differences in DCM parameters between the first (b-s1) and
219 last (b-s5) NF session and considered a model consisting of six motor regions with bidirectional
220 connections among them all (PMCL, PMCR, SMA_L, SMA_R, M1_L, and M1_R). These regions were selected on
221 the basis of the evidence of their role in MI and previous connectivity stroke studies [4], [14], [53]. In
222 this study we focused on endogenous connectivity analysis (DCM matrix A) [49] and assessed how its
223 strength is modulated by the NF training.

224 In the first step of the analysis, a Bayesian model selection procedure for each subject was performed
225 to estimate the model that best matched the measured fMRI data. The basic 6 ROIs model was
226 elaborated into 10 more different models depending upon which premotor region (SMA and PMC) was
227 modulated by the external experimental input (NF task) and a 'null' model with no modulation. The
228 different models (represented in Figure S6 in Supplementary Material) were compared and an optimal
229 DCM model for each subject and session was identified using the Bayesian model selection.

230 After all DCM models were estimated and every subject connectivity strengths was inferred, we
231 performed a group level analysis to assess differences and commonalities between patients using the
232 recently introduced Parametrical Empirical Bayes (PEB) approach [54]. To test hypotheses about
233 between-subjects effects, individual differences in coupling parameters are decomposed into
234 hypothesized group level effects, called regressors or covariates, and unexplained variance or random
235 effects. Since the aim of this study was to assess the effect of the NF training on the EC strength, we
236 introduce this covariate of interest in the PEB analysis. In order to exclude other factors independent
237 from the training, the Fugl-Meyer score, FA asymmetry index, type of stroke and time from stroke were
238 also included as regressors in the between-subjects analysis. We applied PEB to each model and
239 extracted the free energy, which is an approximation of the log-evidence of the model that considers
240 both accuracy and complexity [52], compared them and selected a winning model. The winning model
241 was then considered for the posterior analysis and the group level results. Note that while in first level
242 analysis individual connectivity models are estimated for each patient, the group level PEB analysis
243 assumes a unique model for all the subjects. The estimation of a unique "winning" model enables us to
244 test hypotheses about the common experimental effects on the connectivity strength of the population.

245 Finally, after having identified the winning model, an automatic search over reduced models was
246 performed by means of Bayesian Model Reduction (BMR) [54]. To summarize the results over all the
247 models, a Bayesian Model Average (BMA) was computed [55] by averaging the parameters from

248 different reduced models, weighted by the model posterior probabilities. When showing summary BMA
249 results, we only considered parameters with a strong evidence (i.e. posterior probability of being non-
250 zero greater than 0.99). All the computations were performed using the DCM analysis code adapted
251 from SPM12, described step-by-step in [49], [56] and available at [https://github.com/pzeidman/dcm-](https://github.com/pzeidman/dcm-peb-example)
252 [peb-example](https://github.com/pzeidman/dcm-peb-example). Other scripts used for fMRI and DCM analysis in this paper can be provided by the authors
253 upon request. More details about code availability are also given in Supplementary Material.

254 **Results**

255 Despite the demanding and intensive training protocol, no drops-out were registered: participants
256 found the training satisfying and completed it.

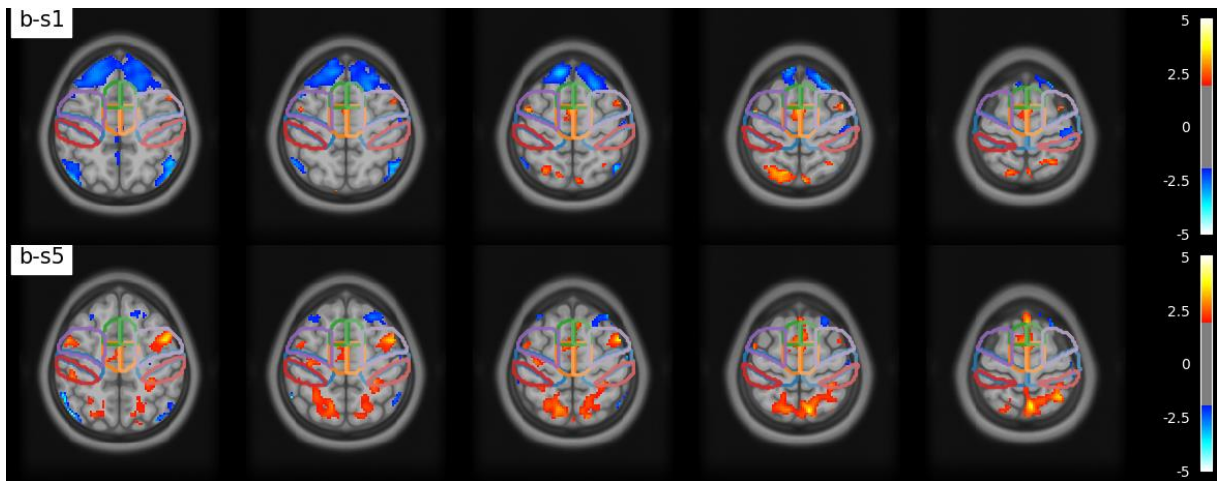
257 *fMRI activation analysis*

258 Even if a thorough analysis of changes in changes in BOLD activation patterns is outside the main scope
259 of this work, which focuses on effective connectivity changes after NF training, we summarize in this
260 paragraph main results. More details about fMRI analysis and additional results are provided in the
261 Supplementary Material.

262 The motion artifacts analysis revealed that in 5 out of 45 training sessions the percentage of head
263 motion outliers was higher than 10%. Also, in 11% of sessions (6 out of 45) the Pearson correlation
264 between the head motion and the NF task regressor was higher than 0.25 (in absolute value). These
265 findings are similar to those reported in a previous study on 30 healthy volunteers [57]. Additional
266 details and results of the offline data quality check are given in Supplementary Material (Table S1 and
267 Figures S1 and S2).

268 Figure 1 presents group activation maps (N=9) in the first (b-s1) and last (b-s5) NF training session, that
269 were then considered for DCM analysis. Reported statistical maps show activations exceeding a voxel-
270 level uncorrected threshold of $p < 0.001$. Average BOLD activation maps show significant activations of
271 the premotor cortex and supplementary motor areas. The bilateral posterior parietal cortex (PPC), that
272 plays an important role in visuo-motor coordination [58], was also recruited during the MI NF task. In
273 general, patients robustly activated mainly the bilateral SMA during the first session (b-s1), while they
274 showed also activation of the bilateral PMC and ipsilesional M1 in the last NF session (b-s5).

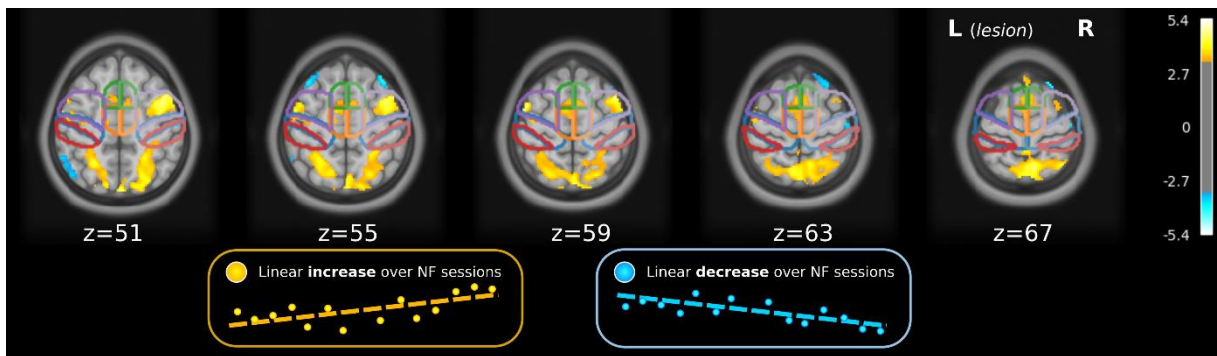
275 Together with differences between the first and last NF session, we also investigated if there was a
276 significant linear increase of BOLD activation across the 14 NF runs of the five bimodal sessions. Group
277 results in Figure 2 suggest that bilateral SMA and PMC BOLD activation linearly increased from one
278 session to another (clusters of $k > 25$ voxels, $p < 0.001$, uncorrected). A localized increase could be
279 observed also in the ipsilesional M1, but did not correspond to an increase in the contralesional M1.
280 Individual maps indicate that activation patterns across patients are variable, even if a linear increase in
281 activation of SMA and PMC can be observed in the majority of the individuals (Figure S4a). Similarly, the
282 analysis of offline NF scores for SMA and M1 indicated that a significant increase in the average SMA NF
283 score was observed in the majority of patients, while results concerning M1 NF scores are more variable
284 across individuals (Figure S4a and S4b).



285

286 *Figure 1. Group activation maps in the first (b-s1) and last (b-s5) training session in MNI coordinates ($p < 0.05$,
 287 uncorrected). The outline of the motor areas of interest based on the HMAT atlas is indicated: preSMA (green) SMA
 288 (orange), PMC (purple), M1 (blue) and Sensory motor cortex (red). The lesional hemisphere is on the left (results
 289 for the patients whose lesion was in the right hemisphere were flipped for the sake of comparison).*

290



291

292 *Figure 2. BOLD activation linear increase along NF sessions. Cluster of voxels ($k > 25$) exhibiting a significant linear
 293 increase (decrease) over the 14 bimodal NF runs are showed in yellow (light blue) ($p < 0.001$, uncorrected). The
 294 outline of the motor areas of interest based on the HMAT atlas is indicated: preSMA (green) SMA (orange), PMC
 295 (purple), M1 (blue) and Sensory motor cortex (red). The lesional hemisphere is on the left (results for the patients
 296 whose lesion was in the right hemisphere were flipped for the sake of comparison).*

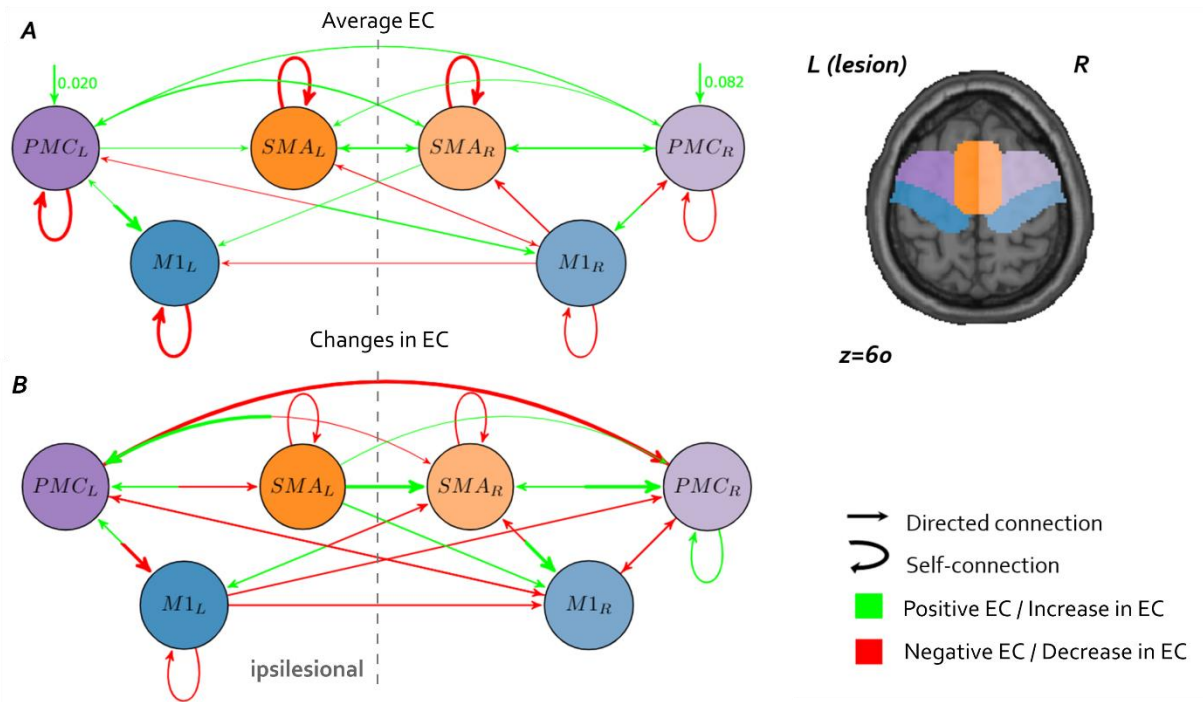
297 *DCM analysis: changes in endogenous connectivity*

298 The subject average percentage variance explained by the model is 10.5% (SD 7.3%): it compares to
 299 other results in literature [49] but is smaller. This is to be expected in the case of simultaneous EEG-
 300 fMRI imaging considered the decrease in fMRI signal to noise ratio due to the presence of EEG
 301 electrodes [59]. In most of the subjects, coupling parameters were non-trivial, with 90% credible
 302 intervals that excluded zero, indicating that there was useful information in the data pertaining to the
 303 NF experimental effects. The PEB free energy, considered to be a proxy for the log model evidence, was
 304 of -1.012×10^5 (a graph reporting the free energy corresponding to the 10 DCM models is reported
 305 in Supplementary Material, Figure S7).

306 Endogenous connectivity patterns elicited during MI NF obtained from the BMA analysis are
 307 schematically represented in Figure 3 and the corresponding values are listed in Table 2. Coupling

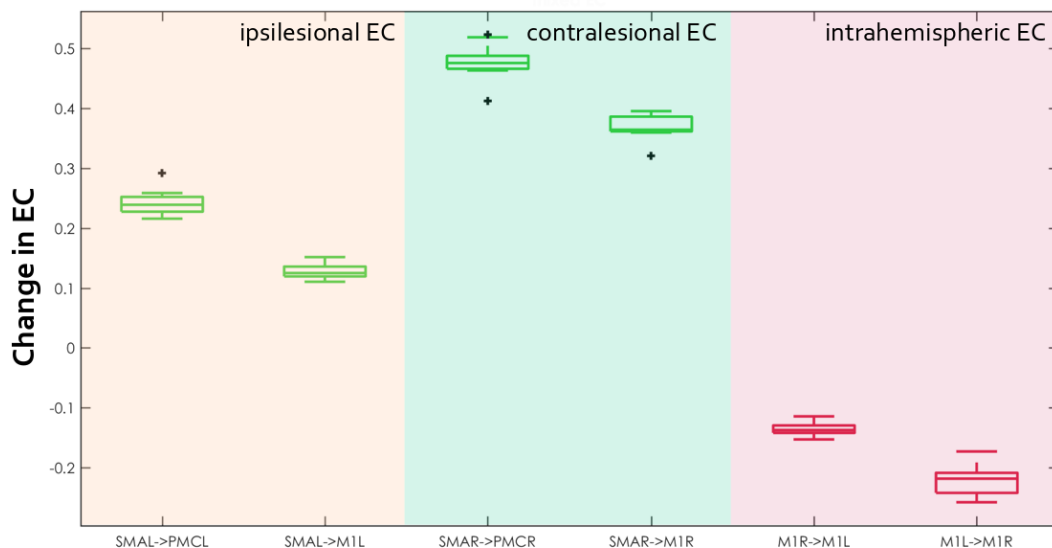
308 parameters in average connectivity patterns (i.e. common to all subjects and sessions) quantify the EC
309 from one area over another in Hz. Negative coupling rates indicate that the source region has an
310 inhibitory effect on the activity of the target region (in red in Figure 3), while positive EC values indicate
311 an excitatory effect (in green in Figure 3). Inhibitory self-connections scale up or down the default value
312 of 0.5 Hz [49] therefore positive self-connection values indicate increased self-inhibition while negative
313 values indicate activation of the specific region. As shown in Figure 3A, experimental driving inputs (NF
314 MI task) had a positive influence on bilateral premotor areas: this is consistent with the recruitment of
315 PMC during a MI task [60]. The average EC results indicate a fully connected motor network, with mainly
316 excitatory coupling, involving both hemispheres. Connectivity between contralesional and ipsilesional
317 motor areas was also elicited during the MI task of the affected limb. Self-connection values were
318 negative for all ROIs, indicating a significant disinhibition, or equivalently an activation, of all the
319 considered motor regions during the NF MI task.

320 In Figures 3B and 4 modulatory effects of the NF training on EC strength are represented, with positive
321 connections (green) indicating an average increase in connectivity between ROIs and negative
322 connections (red) representing a decrease in EC between the first and last NF training session. A general
323 trend of decrease in inter-hemispheric connectivity strength can be observed, in particular between
324 contralesional (right) and ipsilesional (left) PMC and M1. Only connections originating from SMA
325 towards the M1 and PMC increased in strength following the NF training, while feedback connectivity
326 from ipsilesional M1 to all other motor areas was reduced (except for the connection to ipsilesional PMC
327 that increased). A decrease in self-inhibition strength in bilateral SMA and ipsilesional M1 was observed:
328 this indicates a higher activation of these regions as a result of training, in line with the results of the
329 whole brain analysis presented in Figures 1 and 2. In order to assess the variability in connectivity
330 strength changes across subjects, we calculated the difference between individual endogenous
331 connectivity (matrices A) in b-s1 and b-s5. Representative results for six connections (ipsilesional,
332 contralesional and intrahemispheric EC) are shown in Figure 4 and indicate consistent findings:
333 individual connectivity strength have the same signs and similar amplitudes across patients. Additional
334 results can be found in Figures S5 and S6.



335

336 *Figure 3. Bayesian Model Average (BMA) results. A. Connectivity network commonalities across subjects and*
 337 *training sessions. Arrows thickness and color code respectively for the strength and the sign of EC: green arrows*
 338 *represent a positive (excitatory) coupling, while red arrows indicate negative coupling. B. Significant changes*
 339 *($p < 0.01$) in EC strength after the NF training. Arrows thickness and color code respectively for the strength and the*
 340 *sign of EC change: green arrows represent an increase in connectivity, while red arrows indicate a decrease. The*
 341 *direction of links is represented by the arrow's ending. Since EC is not symmetrical, an opposite change in*
 342 *connectivity can be observed between two regions. It is the case of regions connected by a "bicolor" arrow (i.e. in*
 343 *panel B the arrow between $M1_L$ and PMC_L indicate an increase of the connectivity from $M1_L$ to PMC_L and a decrease*
 344 *of connectivity from PMC_L to $M1_L$).*



345

346 *Figure 4. Changes in EC connectivity across patients for six representative connections. Boxplots indicate the*
 347 *median (central mark) and the 25th and 75th percentiles (bottom and top edges of the box) of the EC changes*
 348 *across 9 patients. Outliers are shown with a black cross. Green boxplots correspond to an increase in connectivity*
 349 *strength from b-s1 to b-s5; inversely red boxplots correspond to a decrease in EC after NF training.*

350 *Table 1. Patients demographic and stroke characteristics.*

Patient ID	Gender	Time from stroke (months)	Stroke type	Stroke lesion	Fugl-Meyer	FA_asymmetry
P01	F	25	Ischemic, middle left cerebral artery	Left	53	0.0257
P02	M	34	Ischemic, middle left cerebral artery	Left	50	0.0180
P03	M	68	Subcortical haemorrhagic stroke	Right	26	0.12
P04	M	49	Ischemic, middle left cerebral artery	Left	29	0.0590
P05	M	28	Ischemic, middle left cerebral artery	Left	39	0.002
P06	M	199	Left haemorrhagic	Left	26	0.124
P07	M	36	Ischemic, middle left cerebral artery	Left	42	-0.008
P08	F	26	Ischemic, middle right cerebral artery	Right	55	0.001
P09	F	14	Ischemic, middle right cerebral artery	Right	52	0.098

351

352 *Table 2. Bayesian Model Average of PEB parameters: Average endogenous connectivity and significant changes in*
 353 *connectivity strength as a result of the NF training.*

Source	Target	Commonalities	Effect of Treatment
SMA _L	SMA _L	-0.3616	-0.1339
SMA _L	PMC _L	-0.0000	0.0893
SMA _L	M1 _L	-0.0000	0.0000
SMA _L	SMA _R	0.2396	0.1784
SMA _L	PMC _R	0.0000	0.0856
SMA _L	M1 _R	-0.0902	0.1140
PMC _L	SMA _L	0.1077	-0.1608
PMC _L	PMC _L	-0.4562	0.0000
PMC _L	M1 _L	0.3510	-0.2343
PMC _L	SMA _R	0.0904	-0.0808
PMC _L	PMC _R	0.1367	-0.1872
PMC _L	M1 _R	0.2282	-0.1034
M1 _L	SMA _L	0.0000	0.0000
M1 _L	PMC _L	0.0860	0.0890
M1 _L	M1 _L	-0.3818	-0.1635
M1 _L	SMA _R	0.0000	-0.1213
M1 _L	PMC _R	0.0000	-0.0995
M1 _L	M1 _R	0.0000	-0.0974
SMA _R	SMA _L	0.1752	0.0460
SMA _R	PMC _L	0.2006	0.1830
SMA _R	M1 _L	0.0830	0.1711
SMA _R	SMA _R	-0.3444	-0.1195
SMA _R	PMC _R	0.2365	0.2620
SMA _R	M1 _R	0.0000	0.1753
PMC _R	SMA _L	0.1227	0.0000
PMC _R	PMC _L	0.0818	-0.1786
PMC _R	M1 _L	0.0000	-0.0000
PMC _R	SMA _R	0.2782	0.0876
PMC _R	PMC _R	-0.2467	0.1195
PMC _R	M1 _R	0.2232	-0.1084
M1 _R	SMA _L	-0.0972	-0.0000
M1 _R	PMC _L	-0.1026	-0.1469
M1 _R	M1 _L	-0.0783	0.0000
M1 _R	SMA _R	-0.2783	-0.1223
M1 _R	PMC _R	-0.1689	-0.1324
M1 _R	M1 _R	-0.2707	0.0000

354

355 **Discussion**

356 We applied a DCM analysis to task-based fMRI data to describe the effect of NF training on bilateral
 357 motor networks in nine chronic stroke patients. The training protocol included five bimodal EEG-fMRI
 358 NF and nine EEG-NF sessions over five weeks aiming at reinforcing the activity of specific motor areas
 359 (ipsilesional SMA and M1). Results indicate that NF training induced a modulation of fMRI activation
 360 during the NF MI task towards ipsilesional motor cortex activation. We also found a reorganization of

361 effective connectivity after training, with a general trend to reduced inter-hemispheric connectivity
362 between premotor and primary motor cortices. These exploratory results suggest that the training of
363 specific motor areas with NF can have an impact overall motor connectivity network.

364 *Methods*

365 Different estimators of EC from fMRI data are available [61]. In this study, we used DCM for EC
366 estimation because it was specifically developed for fMRI analysis. DCM has the advantage over
367 approaches such as structural equation modeling or Granger causality that it uses a hemodynamic
368 model to decompose the measured data into underlying neuronal signal and hemodynamic effects [50].
369 Moreover, DCM is particularly robust in dealing with deviations from the standard hemodynamic
370 response (*e.g.* due to pathology affecting blood flow parameters such as stroke), as the parameters in
371 the hemodynamic model are estimated together with the parameters quantifying neuronal connectivity
372 and individually for each ROI [50], [51]. In the definition of the *a priori* model of underlying connectivity
373 patterns, we considered six regions of interest including both ipsilesional and contralesional premotor
374 and motor areas. Other areas importantly involved in motor network (*i.e.* cerebellum, prefrontal areas)
375 were excluded from the analysis as in DCM models including more than 8 ROIs, additional prior
376 constraints are needed to reduce the number of parameters to estimate [62]. Moreover, DCM analysis
377 does not result in erroneous estimations when regions that may have an influence on the model are
378 disregarded, because information by brain regions not explicitly modelled is captured implicitly in the
379 coupling parameters between two regions [63].

380 *fMRI activation and effective connectivity during a NF-MI task*

381 Group level fMRI results yield activations of the areas typically involved during a NF MI task: SMA, PMC
382 and posterior parietal cortex (PPC) [64]. These results are also in line with findings indicating that PPC is
383 generally active when feedback is presented visually [65]. Activation patterns evolved from the first
384 session to the last of the training. The first session involved SMA and the last session showed a larger
385 recruitment of bilateral PMC and also a localized activation of ipsilesional M1. The activation of bilateral
386 SMA and ipsilesional M1 during the NF task linearly increased across the 14 training runs, indicating
387 that, in average, patients successfully upregulated the targeted cortical areas. When looking at the
388 individual results (see Figure S3), this linear increase is observed in 6 out of 9 patients. However, this
389 type of analysis only reveal significant changes in a linear fashion, and is not able to quantify less gradual,
390 abrupt changes in activation with time. Moreover, caution must be employed in interpreting these
391 results as a direct indicator of the efficacy of the NF training, considered the lack of blinded assessment
392 and the absence of a comparison with a control group.

393 SMA is robustly activated during MI [66] and has been associated to complex MI tasks, involving a
394 sequence of movements [64]. Whether M1 is consistently activated during a MI task is debated.
395 Functional MRI NF studies found non-conclusive results at group level [41], [42] and one recent work
396 reported deactivation of M1 during MI training of the SMA and M1 [66]. A recent meta-analysis only
397 reported consistent activation within the primary motor cortex during MI in a minority of studies (18%)
398 [64]. The authors of this study suggest that only skilled MI performer may be able to activate M1 during
399 a MI task, as found for instance by Sharma et al. [67], which could explain why M1 activation can be
400 more consistently reported in single-subject analyses [68]. Our results indicated an activation of
401 ipsilesional M1 in the last NF session suggesting on the one hand that patients “responded” to the NF

402 reinforcement scheme targeting ipsilesional M1, and on the other that they became better at
403 performing the MI task, which is to be expected after 14 motor NF training sessions.

404 Average connectivity results are in line with previous studies investigating EC patterns in stroke during
405 MI or execution. They indicate a dense, bilateral connectivity pattern, with an inhibitory connection
406 between contralateral M1 and ipsilesional M1. Connectivity in the contralesional hemisphere is
407 commonly elicited in stroke patients during MI of the affected limb and there is evidence that the
408 inhibitory influence from contralesional M1 to ipsilesional M1 increases in stroke patients with respect
409 to healthy controls [13]. The role of contralesional M1 in stroke is debated as it has been shown to have
410 both promoting and inhibitory influences on motor outcomes, depending on the severity and time from
411 stroke[69]–[71]. For instance, a suppression of the contralesional M1 excitability has been shown to
412 degrade upper limb control in severely impaired patients but to improve it for mildly impaired stroke
413 patients [72].

414 *Effect of NF training on effective connectivity*

415 Few recent studies have revealed the potential of modulating functional connectivity between the
416 ipsilesional motor cortex and other cortical [34] or subcortical regions [33] for stroke rehabilitation. In
417 a study involving 10 chronic stroke patients, an enhancement of the functional connectivity FC of
418 preserved ipsilesional motor areas with NF led to a significant increase in motor function. This was not
419 the case in a control condition where patients enhanced FC of a brain area not directly implicated in
420 motor function [34]. However, to the best of our knowledge, this is the first work that assesses fMRI
421 connectivity changes resulting from the NF training of target motor areas in stroke. More generally, this
422 work tackles the need to investigate how NF training of localized activity affects the related brain
423 networks to guide more effective NF strategies based on physiologically relevant network targets and
424 to gain a deeper insight into the underlying pathological processes [73].

425 DCM analysis revealed significant changes in EC after NF training relative to baseline. Firstly, a general
426 decrease in inter-hemispheric connections was observed, including a decrease in the inhibitory
427 influence of the contralesional M1 on the ipsilesional PMC. This inhibitory influence through
428 transcallosal connections reduces the motor output of the damaged hemisphere in patients with severe
429 motor deficit [4], [74], [75], and is part of a well-known “maladaptive” plasticity mechanism in stroke
430 [76]. In a DCM study from Grefkes and colleagues on the effect of transcranial magnetic stimulation
431 applied on contralesional M1, the negative coupling from contralesional M1 was absent as a result of
432 the treatment, and, more interestingly, this effect correlated with improvement in motor performance
433 of the paretic hand [4]. Caution is however recommended when interpreting changes in contralesional
434 M1 connectivity because, even if its alterations in stroke are well-documented, their influence on motor
435 recovery is debated and insufficiently understood [1].

436 We observed an increase in feedforward connectivity strength between ipsilesional SMA and PMC after
437 the NF training. Using a similar BMA approach, Bajaj and colleagues compared the connectivity before
438 and after mental practice and physical therapy intervention [14]. In line with our findings, they reported
439 an increase in EC between SMA and PMC in the affected hemisphere during MI task and this increase
440 was significantly correlated with the motor score improvement after treatment. Similarly, Sharma and
441 colleagues reported that coupling between PMC and SMA is diminished in stroke patients with respect
442 to healthy controls and that as motor function improved, the coupling between these areas increased
443 [77].

444 The general reduction of connectivity from ipsilesional to contralesional motor areas (see also Figure S8
445 in Supplementary Material) suggests a pattern closer to a unilateral motor imagery network in healthy
446 subjects, as the inhibitory influence from M1 to the contralateral motor areas is a well described
447 mechanism of unilateral hand movements [70]. Moreover, an increase in the inhibitory coupling from
448 M1 to SMA and, inversely, a positive coupling from SMA to M1 corresponds to the feed-forward
449 connectivity model estimated with DCM in healthy controls in [78]. More generally, the observed trend
450 of reduction in connectivity can be also interpreted as an effect of learning. Average EC patterns show
451 a fully connected bilateral network during MI (Figure 4A): a decrease in the strength of EC suggests that
452 the same MI task could be performed with a less dense network at the end of the NF training. A similar
453 trend was observed in connectivity patterns during language prosody NF training where connectivity
454 was reduced and more localized at the end of the training [79].

455 Finally, the decrease in self-inhibitory connections in ipsilesional M1 and bilateral SMA indicates that
456 these regions were more activated at the end of the NF training. As results in Table 2 indicate, the largest
457 change was observed in the ipsilesional M1 (-0.1635), followed by ipsilesional SMA (-0.1339) and
458 contralesional SMA (-0.1195). This is in line with the results of the fMRI activation analysis and, more
459 interestingly, with the NF reinforcement scheme that rewarded upregulation of ipsilesional SMA and
460 M1 that rewarded upregulation of ipsilesional SMA and M1, with a shift towards M1 activation at the
461 end of the training.

462 *Future work*

463 The population of this study is relatively small and includes stroke patients with a relatively broad range
464 of stroke latency and lesions localization. Individual motor and structural impairment differences
465 following stroke might induce variability to the estimation of EC with DCM. Unfortunately, this is the
466 case of the majority of fMRI-NF studies, whose sample size is strongly limited by the cost and burden of
467 MRI imaging and also true in this case, considered the technical challenge of bimodal EEG-fMRI NF and
468 the fact that patients underwent a long training program of 14 NF sessions over 5 weeks. We designed
469 this experimental protocol with the rationale that NF training induced changes in brain organization
470 would require a significant amount of training. In future, a larger sample of patients will be considered
471 to refine our findings of NF training effect on connectivity networks and extend our observations. For
472 instance in this first study we only examined changes in connectivity at the end of the training protocol.
473 In future work and on a larger cohort we aim to assess if changes in connectivity occur also after a few
474 NF training sessions with finer granularity.

475 In this exploratory study, we assessed changes in EC estimated from fMRI as it allows for a finer analysis
476 of different motor areas (SMA, PMC and M1) as compared to EEG. In addition, we did not disentangle
477 the role of unimodal EEG and bimodal EEG-fMRI NF in the observed EC changes, as we first assessed if
478 global effect of the NF training on EC could be observed. Future analyses will address these open
479 questions, notably looking at EEG connectivity. Building on these first results, in future work we will also
480 assess if the connectivity changes elicited by NF training resulted in improved motor performance of
481 the affected limb, taking clinical outcomes into account. In order to assess the specific effect of NF
482 training these results needs to be extended with a randomized controlled study, where network
483 reorganization patterns could be compared between the interventional and control group.

484 Overall, we believe that this work represents a valuable and novel analysis of the large-scale effects of
485 localized NF training on fMRI connectivity, and, to the best of our knowledge, the first in stroke. It

486 underlines the importance of investigating also connectivity patterns rather than focusing on regional
487 activation when assessing NF training outcomes.

488 **Conclusions**

489 Using a DCM approach, in this work we investigate the effect of multi-session EEG-fMRI NF training on
490 connectivity patterns in chronic stroke patients. The DCM model consisted in a bilateral motor network
491 including premotor, supplementary and primary motor areas and a Bayesian Model Average approach
492 was used to assess significant changes in connectivity following the NF training. Results show that
493 upregulation of ipsilesional M1 and SMA modulates fMRI activity and effective connectivity in both
494 hemispheres and generally reduces inter-hemispheric connectivity strength. Our results suggest that
495 the upregulation of target motor areas by means of NF can have a larger scale impact on connectivity
496 and a potential to mitigate maladaptive networks patterns.

497

498 **Acknowledgements**

499 MRI data acquisition was supported by the Neurinfo MRI research facility from the University of Rennes
500 I. Neurinfo is granted by the the European Union (FEDER), the French State, the Brittany Council, Rennes
501 Metropole, Inria, Inserm and the University Hospital of Rennes. We thank Gabriela Vargas for her useful
502 suggestions for the DCM analysis. The project was supported by the National Research Agency in the
503 “Investing for 540 the Future” program under reference ANR-10-LABX-07-0, and by the “Fondation pour
504 la Recherche Médicale” under the convention #DIC20161236427.

505

506 **Author contributions**

507 G.L. wrote the manuscript, A.V. and Q.D. contributed to methods section writing. G.L., I.B., S.B., C.B. and
508 A.L. designed the studies. I.B., S.B. and E.L. contributed to patient enrollment and screening. A.V., G.L.,
509 J.C. and Q.D. performed the data analysis. G.L., E.L. and M.F. collected the data. G.L. and E.B. contributed
510 to the design of the experimental platform. All authors reviewed the manuscript.

511

512 **References**

- 513 [1] A. G. Guggisberg, P. J. Koch, F. C. Hummel, and C. M. Buetefisch, “Brain networks and their
514 relevance for stroke rehabilitation,” *Clin. Neurophysiol.*, vol. 130, no. 7, pp. 1098–1124, 2019.
- 515 [2] H. Johansen-Berg, J. Scholz, and C. J. Stagg, “Relevance of structural brain connectivity to
516 learning and recovery from stroke,” *Front. Syst. Neurosci.*, vol. 4, no. November 2010, 2010.
- 517 [3] A. K. Rehme, S. B. Eickhoff, L. E. Wang, G. R. Fink, and C. Grefkes, “Dynamic causal modeling of
518 cortical activity from the acute to the chronic stage after stroke,” *Neuroimage*, vol. 55, no. 3,
519 pp. 1147–1158, 2011.
- 520 [4] C. Grefkes *et al.*, “Cortical Connectivity after Subcortical Stroke Assessed with Functional
521 Magnetic Resonance Imaging,” *Ann. Neurol.*, vol. 63, pp. 236–246, 2008.
- 522 [5] H. Johansen-Berg, M. F. S. Rushworth, M. D. Bogdanovic, U. Kischka, S. Wimalaratna, and P. M.
523 Matthews, “The role of ipsilateral premotor cortex in hand movement after stroke,” *Proc. Natl.
524 Acad. Sci. U. S. A.*, vol. 99, no. 22, pp. 14518–14523, 2002.

- 525 [6] M. Catani and D. H. Ffytche, "The rises and falls of disconnection syndromes," *Brain*, vol. 128,
526 no. 10, pp. 2224–2239, 2005.
- 527 [7] W. de Haan, K. Mott, E. C. W. van Straaten, P. Scheltens, and C. J. Stam, "Activity Dependent
528 Degeneration Explains Hub Vulnerability in Alzheimer's Disease," *PLoS Comput. Biol.*, vol. 8, no.
529 8, 2012.
- 530 [8] A. Fornito, A. Zalesky, and M. Breakspear, "The connectomics of brain disorders," *Nat. Rev.*
531 *Neurosci.*, vol. 16, no. 3, pp. 159–172, 2015.
- 532 [9] N. S. Ward, M. M. Brown, A. J. Thompson, and R. S. J. Frackowiak, "Neural correlates of motor
533 recovery after stroke : a longitudinal fMRI study," vol. 126, no. 0 11, pp. 2476–2496, 2013.
- 534 [10] N. S. Ward, "Future perspectives in functional neuroimaging in stroke recovery," *Eura*
535 *Medicophys*, vol. 43, pp. 285–294, 2007.
- 536 [11] N. Sharma, J. Baron, and J. B. Rowe, "Motor Imagery After Stroke : Relating Outcome to Motor
537 Network Connectivity," *Ann. Neurol.*, vol. 66, no. 5, pp. 604–616, 2009.
- 538 [12] A. Lazaridou *et al.*, "fMRI as a molecular imaging procedure for the functional reorganization of
539 motor systems in chronic stroke," *Mol. Med. Rep.*, vol. 8, no. 3, pp. 775–779, 2013.
- 540 [13] C. Grefkes and G. R. Fink, "Reorganization of cerebral networks after stroke: New insights from
541 neuroimaging with connectivity approaches," *Brain*, vol. 134, no. 5, pp. 1264–1276, 2011.
- 542 [14] S. Bajaj, A. J. Butler, D. Drake, and M. Dhamala, "Brain effective connectivity during motor-
543 imagery and execution following stroke and rehabilitation," *NeuroImage Clin.*, vol. 8, pp. 572–
544 582, 2015.
- 545 [15] K. J. Friston, "Functional and effective connectivity: a review.," *Brain Connect.*, vol. 1, no. 1, pp.
546 13–36, Jan. 2011.
- 547 [16] L. Wang *et al.*, "Dynamic functional reorganization of the motor execution network after
548 stroke," *Brain*, vol. 133, no. 4, pp. 1224–1238, 2010.
- 549 [17] F. De Vico Fallani *et al.*, "Evaluation of the brain network organization from EEG signals: A
550 preliminary evidence in stroke patient," *Anat. Rec.*, vol. 292, no. 12, pp. 2023–2031, 2009.
- 551 [18] L. Wang, J. Zhang, Y. Zhang, R. Yan, H. Liu, and M. Qiu, "Conditional Granger Causality Analysis
552 of Effective Connectivity during Motor Imagery and Motor Execution in Stroke Patients,"
553 *Biomed Res. Int.*, vol. 2016, 2016.
- 554 [19] C. Grefkes, D. A. Nowak, L. E. Wang, M. Dafotakis, S. B. Eickhoff, and G. R. Fink, "Modulating
555 cortical connectivity in stroke patients by rTMS assessed with fMRI and dynamic causal
556 modeling," *Neuroimage*, vol. 50, no. 1, pp. 233–242, 2010.
- 557 [20] S. M. Smith *et al.*, "Network modelling methods for FMRI," *Neuroimage*, vol. 54, no. 2, pp. 875–
558 891, 2011.
- 559 [21] M. A. Cervera *et al.*, "Brain-Computer Interfaces for Post-Stroke Motor Rehabilitation: A Meta-
560 Analysis," *bioRxiv*, pp. 1–22, 2017.
- 561 [22] F. Pichiorri *et al.*, "Sensorimotor rhythm-based brain-computer interface training: The impact
562 on motor cortical responsiveness," *J. Neural Eng.*, vol. 8, no. 2, 2011.
- 563 [23] T. Wang, D. Mantini, and C. R. Gillebert, "The potential of real-time fMRI neurofeedback for
564 stroke rehabilitation," *Cortex*, no. S0010-9452(17)30301–5, 2017.
- 565 [24] G. Lioi *et al.*, "A multi-target motor imagery training using bimodal EEG-fMRI Neurofeedback: a

- 566 pilot study on chronic stroke patients," *Front. Hum. Neurosci.*, vol. 14, no. February, pp. 1–13,
567 2020.
- 568 [25] D. E. J. Linden and D. L. Turner, "Real-time functional magnetic resonance imaging
569 neurofeedback in motor neurorehabilitation," *Curr. Opin. Neurol.*, vol. 29, no. 4, pp. 412–418,
570 2016.
- 571 [26] C. Zich, S. Debener, C. Kranczioch, M. G. Bleichner, I. Gutberlet, and M. De Vos, "Real-time EEG
572 feedback during simultaneous EEG-fMRI identifies the cortical signature of motor imagery,"
573 *Neuroimage*, vol. 114, pp. 438–447, 2015.
- 574 [27] E. Bagarinao *et al.*, "Improved volitional recall of motor-imagery-related brain activation
575 patterns using real-time functional MRI-based neurofeedback," *Front. Hum. Neurosci.*, vol. 12,
576 no. April, pp. 1–13, 2018.
- 577 [28] A. Ramos-Murguialday *et al.*, "Brain-Machine-Interface in Chronic Stroke Rehabilitation: A
578 Controlled Study," *Ann. Neurol.*, vol. 74, no. 1, pp. 100–108, 2014.
- 579 [29] M. Fleury *et al.*, "A Survey on the Use of Haptic Feedback for Brain-Computer Interfaces and
580 Neurofeedback," *Front. Hum. Neurosci.*, 2020.
- 581 [30] C. Jeunet, B. Glize, A. McGonigal, J. M. Batail, and J. A. Micoulaud-Franchi, "Using EEG-based
582 brain computer interface and neurofeedback targeting sensorimotor rhythms to improve
583 motor skills: Theoretical background, applications and prospects," *Neurophysiol. Clin.*, 2018.
- 584 [31] F. Pichiorri *et al.*, "Brain-computer interface boosts motor imagery practice during stroke
585 recovery," *Ann. Neurol.*, vol. 77, no. 5, pp. 851–865, 2015.
- 586 [32] C. Zich, "High intensity chronic stroke motor imagery neurofeedback training at home - three
587 case reports," *Clin. EEG Neurosci.*, 2017.
- 588 [33] S.-L. Liew *et al.*, "Improving Motor Corticothalamic Communication After Stroke Using Real-
589 Time fMRI Connectivity-Based Neurofeedback," *Neurorehabil. Neural Repair*, vol. 30, no. 7, pp.
590 671–675, 2016.
- 591 [34] A. Mottaz *et al.*, "Modulating functional connectivity after stroke with neurofeedback: Effect on
592 motor deficits in a controlled cross-over study," *NeuroImage Clin.*, vol. 20, no. July, pp. 336–
593 346, 2018.
- 594 [35] R. Sitaram *et al.*, "Acquired control of ventral premotor cortex activity by feedback training: An
595 exploratory real-time fMRI and TMS study," *Neurorehabil. Neural Repair*, vol. 26, no. 3, pp.
596 256–265, 2012.
- 597 [36] K. D. Young, V. Zotev, R. Phillips, M. Misaki, H. Yuan, and W. C. Drevets, "Real-Time fMRI
598 Neurofeedback Training of Amygdala Activity in Patients with Major Depressive Disorder," *PLoS*
599 *One*, vol. 9, no. 2, p. e88785, 2014.
- 600 [37] V. Zotev, R. Phillips, H. Yuan, M. Misaki, and J. Bodurka, "Self-regulation of human brain activity
601 using simultaneous real-time fMRI and EEG neurofeedback," *Neuroimage*, vol. 85, no. 2014,
602 pp. 985–995, 2014.
- 603 [38] L. Perronnet *et al.*, "Learning 2-in-1 : Towards Integrated EEG-fMRI Neurofeedback," *bioRxiv*,
604 pp. 1–30, 2020.
- 605 [39] C. M. Stinear, P. A. Barber, M. Petoe, S. Anwar, and W. D. Byblow, "The PREP algorithm predicts
606 potential for upper limb recovery after stroke," *Brain*, vol. 135, no. 8, pp. 2527–2535, 2012.
- 607 [40] M. Mano, A. Lécuyer, E. Bannier, L. Perronnet, S. Noorzadeh, and C. Barillot, "How to Build a

- 608 Hybrid Neurofeedback Platform Combining EEG and fMRI," *Front. Neurosci.*, vol. 11, no. 140,
609 2017.
- 610 [41] M. Chiew, S. M. LaConte, and S. J. Graham, "Investigation of fMRI neurofeedback of differential
611 primary motor cortex activity using kinesthetic motor imagery," *Neuroimage*, vol. 61, no. 1, pp.
612 21–31, 2012.
- 613 [42] M. L. Blefari, J. Sulzer, M. C. Hepp-Reymond, S. Kollias, and R. Gassert, "Improvement in
614 precision grip force control with self-modulation of primary motor cortex during motor
615 imagery," *Front. Behav. Neurosci.*, vol. 9, no. FEB, pp. 1–11, 2015.
- 616 [43] R. T. Thibault, A. MacPherson, M. Lifshitz, R. R. Roth, and A. Raz, "Neurofeedback with fMRI: A
617 critical systematic review," *Neuroimage*, vol. 172, no. December 2017, pp. 786–807, 2018.
- 618 [44] T. Ros *et al.*, "Consensus on the reporting and experimental design of clinical and cognitive-
619 behavioural neurofeedback studies (CRED-nf checklist)," *Brain*, vol. 0, pp. 1–12, 2020.
- 620 [45] S. Heunis, R. Lamerichs, S. Zinger, B. Aldenkamp, and M. Breeuwer, "Quality and denoising in
621 real-time fMRI neurofeedback : a methods review," *Open Sci. Framew.*, no. June, 2018.
- 622 [46] J. D. Power, A. Mitra, T. O. Laumann, A. Z. Snyder, B. L. Schlaggar, and S. E. Petersen,
623 "Comparison of fMRI motion correction software tools," *Neuroimage*, vol. 84, pp. 529–543,
624 2014.
- 625 [47] S. Zarrar *et al.*, "The Preprocessed Connectomes Project Quality Assessment Protocol - a
626 resource for measuring the quality of MRI data.," *Front. Neurosci.*, pp. 2–3, 2015.
- 627 [48] M. A. Mayka, D. M. Corcos, S. E. Leurgans, and D. E. Vaillancourt, "Three-dimensional locations
628 and boundaries of motor and premotor cortices as defined by functional brain imaging: A
629 meta-analysis," *Neuroimage*, vol. 31, no. 4, pp. 1453–1474, 2006.
- 630 [49] P. Zeidman *et al.*, "A guide to group effective connectivity analysis, part 1: First level analysis
631 with DCM for fMRI," *Neuroimage*, vol. 200, no. March, pp. 174–190, 2019.
- 632 [50] K. J. Friston, L. Harrison, and W. Penny, "Dynamic causal modelling," *Neuroimage*, vol. 19, no.
633 4, pp. 1273–1302, 2003.
- 634 [51] K. E. Stephan, W. D. Penny, R. J. Moran, H. E. M. den Ouden, J. Daunizeau, and K. J. Friston,
635 "Ten simple rules for dynamic causal modeling," *Neuroimage*, vol. 49, no. 4, pp. 3099–3109,
636 2010.
- 637 [52] K. Friston, J. Mattout, N. Trujillo-Barreto, J. Ashburner, and W. Penny, "Variational free energy
638 and the Laplace approximation," *Neuroimage*, vol. 34, no. 1, pp. 220–234, 2007.
- 639 [53] D. Hermes *et al.*, "Functional MRI-based identification of brain areas involved in motor imagery
640 for implantable brain-computer interfaces," *J. Neural Eng.*, vol. 8, no. 2, 2011.
- 641 [54] K. J. Friston *et al.*, "Bayesian model reduction and empirical Bayes for group (DCM) studies,"
642 *Neuroimage*, vol. 128, pp. 413–431, 2016.
- 643 [55] J. A. Hoeting, D. Madigan, A. E. Raftery, and C. T. Volinsky, "Bayesian Model Averaging: A
644 Tutorial," *Stat. Sci.*, vol. 14, no. 4, pp. 382–417, 1999.
- 645 [56] P. Zeidman *et al.*, "A guide to group effective connectivity analysis, part 2: Second level analysis
646 with PEB," *Neuroimage*, vol. 200, no. May, pp. 12–25, 2019.
- 647 [57] G. Lioi *et al.*, "Simultaneous MRI-EEG during a motor imagery neurofeedback task: an open
648 access brain imaging dataset for multi-modal data integration Authors," *bioRxiv*, 2019.

- 649 [58] E. B. Torres, A. Raymer, L. J. G. Rothi, K. M. Heilman, and H. Poizner, "Sensory-spatial
650 transformations in the left posterior parietal cortex may contribute to reach timing," *J.*
651 *Neurophysiol.*, vol. 104, no. 5, pp. 2375–2388, 2010.
- 652 [59] K. Mullinger, S. Debener, R. Coxon, and R. Bowtell, "Effects of simultaneous EEG recording on
653 MRI data quality at 1.5, 3 and 7 tesla," *Int. J. Psychophysiol.*, vol. 67, no. 3, pp. 178–188, 2008.
- 654 [60] T. Hanakawa, M. A. Dimyan, and M. Hallett, "Motor planning, imagery, and execution in the
655 distributed motor network: A time-course study with functional MRI," *Cereb. Cortex*, vol. 18,
656 no. 12, pp. 2775–2788, 2008.
- 657 [61] J. F. Smith, K. Chen, A. S. Pillai, B. Horwitz, and A. S. Dick, "Identifying effective connectivity
658 parameters in simulated fMRI : a direct comparison of switching linear dynamic system ,
659 stochastic dynamic causal , and multivariate autoregressive models," no. May, pp. 1–17, 2013.
- 660 [62] M. L. Seghier and K. J. Friston, "Network discovery with large DCMs," *Neuroimage*, vol. 68, pp.
661 181–191, 2013.
- 662 [63] K. Friston, "Dynamic causal modeling and Granger causality Comments on: The identification of
663 interacting networks in the brain using fMRI: Model selection, causality and deconvolution,"
664 *Neuroimage*, vol. 58, no. 2, pp. 303–305, 2011.
- 665 [64] S. Héту *et al.*, "The neural network of motor imagery: An ALE meta-analysis," *Neurosci.*
666 *Biobehav. Rev.*, vol. 37, no. 5, pp. 930–949, 2013.
- 667 [65] R. Sitaram *et al.*, "Closed-loop brain training: The science of neurofeedback," *Nat. Rev.*
668 *Neurosci.*, vol. 18, no. 2, pp. 86–100, 2017.
- 669 [66] D. M. A. Mehler *et al.*, "The BOLD response in primary motor cortex and supplementary motor
670 area during kinesthetic motor imagery based graded fMRI neurofeedback," *Neuroimage*, vol.
671 184, pp. 36–44, 2019.
- 672 [67] N. Sharma, P. S. Jones, T. A. Carpenter, and J. C. Baron, "Mapping the involvement of BA 4a and
673 4p during Motor Imagery," *Neuroimage*, vol. 41, no. 1, pp. 92–99, 2008.
- 674 [68] P. Dechent, K. D. Merboldt, and J. Frahm, "Is the human primary motor cortex involved in
675 motor imagery?," *Brain Res. Cogn Brain Res*, vol. 19, no. 2, pp. 138–144, 2004.
- 676 [69] C. Gerloff *et al.*, "Multimodal imaging of brain reorganization in motor areas of the
677 contralesional hemisphere of well recovered patients after capsular stroke," *Brain*, vol. 129, no.
678 3, pp. 791–808, 2006.
- 679 [70] C. Grefkes, S. B. Eickhoff, D. A. Nowak, M. Dafotakis, and G. R. Fink, "Dynamic intra- and
680 interhemispheric interactions during unilateral and bilateral hand movements assessed with
681 fMRI and DCM," *Neuroimage*, vol. 41, no. 4, pp. 1382–1394, 2008.
- 682 [71] D. A. Nowak, C. Grefkes, M. Ameli, and G. R. Fink, "Interhemispheric competition after stroke:
683 Brain stimulation to enhance recovery of function of the affected hand," *Neurorehabil. Neural*
684 *Repair*, vol. 23, no. 7, pp. 641–656, 2009.
- 685 [72] L. V Bradnam, C. M. Stinear, and W. D. Byblow, "Ipsilateral motor pathways after stroke :
686 implications for non-invasive brain stimulation," *Front. Hum. Neurosci.*, vol. 7, no. May, pp. 1–8,
687 2013.
- 688 [73] D. S. Bassett and A. N. Khambhati, "A network engineering perspective on probing and
689 perturbing cognition with neurofeedback," *Ann. N. Y. Acad. Sci.*, pp. 1–18, 2017.
- 690 [74] C. Grefkes and G. R. Fink, "Connectivity-based approaches in stroke and recovery of function,"

- 691 *Lancet Neurol.*, vol. 13, no. 2, pp. 206–216, 2014.
- 692 [75] F. De Vico Fallani *et al.*, “Multiscale topological properties of functional brain networks during
693 motor imagery after stroke,” *Neuroimage*, vol. 83, pp. 438–449, 2013.
- 694 [76] N. Takeuchi and S. I. Izumi, “Maladaptive plasticity for motor recovery after stroke:
695 Mechanisms and approaches,” *Neural Plast.*, vol. 2012, 2012.
- 696 [77] N. Sharma, J. C. Baron, and J. B. Rowe, “Motor imagery after stroke: Relating outcome to motor
697 network connectivity,” *Ann. Neurol.*, vol. 66, no. 5, pp. 604–616, 2009.
- 698 [78] C. H. Kasess, C. Windischberger, R. Cunnington, R. Lanzenberger, L. Pezawas, and E. Moser,
699 “The suppressive influence of SMA on M1 in motor imagery revealed by fMRI and dynamic
700 causal modeling,” *Neuroimage*, vol. 40, no. 2, pp. 828–837, 2008.
- 701 [79] G. Rota, G. Handjaras, R. Sitaram, N. Birbaumer, and G. Dogil, “Reorganization of functional and
702 effective connectivity during real-time fMRI-BCI modulation of prosody processing,” *Brain*
703 *Lang.*, vol. 117, no. 3, pp. 123–132, 2011.
- 704
- 705